Additive Manufacturing 11 (2016) 77–84

Contents lists available at ScienceDirect

Additive Manufacturing

journal homepage: www.elsevier.com/locate/addma

Full length article

Spreading of the nanofluid triple line in ink jet printed electronics tracks☆

Saeid Vafaei[a,b,*], Christopher Tuck[b], Ricky Wildman[c], Ian Ashcroft[b,*]

[a] Department of Mechanical Engineering, Bradley University, IL, USA
[b] Additive Manufacturing and 3D Printing Research Group, EPSRC Centre for Innovative Manufacturing in Additive Manufacturing, Department of Mechanical, Materials and Manufacturing, University of Nottingham, Nottingham, UK
[c] Additive Manufacturing and 3D Printing Research Group, EPSRC Centre for Innovative Manufacturing in Additive Manufacturing, Department of Chemical and Environmental Engineering, University of Nottingham, Nottingham, UK

ARTICLE INFO

Article history:
Received 25 October 2014
Received in revised form
29 November 2015
Accepted 13 April 2016
Available online 21 April 2016

Keywords:
Layering phenomenon
Contact angle
Solid surface tensions
Liquid-gas surface tension
Nanofluids
Young–Laplace equation

ABSTRACT

One of the next avenues for Additive Manufacturing to develop is that of multi-material deposition in order to add functionality to the already complex geometries that are capable of being manufactured. However, for electronic applications the fidelity of the deposited electronic tracks is of utmost importance. The purpose of this study was to investigate the effects of solid surface tensions, $\sigma_{sg} - \sigma_{sl}$, on the quality of printed lines, using 30–40 nm silver nanofluid ink. The solid surface tensions of silver ink on glass and polytetrofluoroethylene (PTFE) substrates were determined theoretically, knowing characteristics of droplet. Meanwhile, a Dimatix printer with nozzles of size of 21.5 μm was used to print conductive lines on smooth glass and PTFE substrates. The printed lines on glass were observed to be continuous with high quality of triple line, which was attributed to the high solid surface tensions of silver nanofluid ink on glass substrates. The solid surface tensions of silver nanofluid ink were relatively low on PTFE, as results the printed lines were discontinuous. The solid surface tensions were introduced as a reliable criterion to predict the printability of nanofluids. The distribution of silver nanoparticles and layering phenomenon in silver nanofluid triple region on glass substrate was clearly observed, using environmental scanning electron microscopy (ESEM) for the first time. In addition to disjoining pressure, the size of droplet and affinity of nanofluid for substrate were observed to have important influences on spreading of nanoparticles in triple region.

1. Introduction

Additive Manufacturing (AM) has reached a point where the development of complex shapes and topologies are now possible in materials that many industrial users can or are beginning to accept. For some the next paradigm of AM is to develop systems and materials that are capable of complex 3D shape with the addition of multiple materials contemporaneously for the addition of function. One such functionality is to add the ability to 'thread' electronics throughout a 3D space encased within dielectric material, however for these materials, normally conductive nanoparticle inks, to have success high fidelity of these tracks is key to their performance. The printing of conductive nanoparticles is attractive due to their potential applications in printed electronic circuits. The direct deposition of conductive lines has a significant influence on the cost and manufacturing of micro devices.

It is also important to maximize the conductivity or minimize the resistance of printed tracks. For a given resistivity, the resistance of a printed track depends on its cross sectional area. Engineering of surface wettability [1] and the behavior of the triple line (triple line is a line that gas, solid and liquid meet each other) are the most effective methods to manipulate the cross sectional area of a printed line. Recently, microstructuring of the substrates has been suggested to modify the wettability and cross sectional area of the printed lines, using nanofluid inks [1].

☆ One of the authors of this article is part of the Editorial Board of the journal. Full responsibility for the editorial and peer-review process for this article lies with the journal's Editor-in-Chief Prof. Ryan Wicker and Deputy Editor Prof. Eric MacDonald. Furthermore, the authors of this article had no and do not currently have access to any confidential information related to its peer-review process.

* Corresponding authors at: Additive Manufacturing and 3D Printing Research Group, EPSRC Centre for Innovative Manufacturing in Additive Manufacturing, Department of Mechanical, Materials and Manufacturing, University of Nottingham, Nottingham, UK.
E-mail addresses: svafaei@fsmail.Bradley.edu (S. Vafaei), ian.ashcroft@nottingham.ac.uk (I. Ashcroft).

http://dx.doi.org/10.1016/j.addma.2016.04.005
2214-8604/

Nomenclature

g	Acceleration of gravity [m/s^2]
R_o	Radius of curvature at apex [m]
R_1,R_2	Radius of curvature [m]
r_d	Radius of contact line [m]
V	Volume [m^3]
Greek Symbols	
δ	Height of apex [m]
θ_e	Equilibrium contact angle [*Deg.*]
ρ_l	Liquid density [kg/m^3]
ρ_g	Gas density [kg/m^3]
σ_{lg}	Liquid-gas surface tension [N/m]
σ_{sg}	Solid-gas surface tension [N/m]
σ_{sl}	Solid-liquid surface tension [N/m]
$\sigma_{lg\,n}$	Liquid-gas surface tension of nanofluids [N/m]

Practically, the behavior of the triple line or wettability mainly depends on the force balance between liquid-gas, σ_{lg}, and solid surface tensions, $\sigma_{sg}-\sigma_{sl}$. In general, for a given injected liquid volume, the triple line moves toward the liquid phase as solid surface tensions, $\sigma_{sg}-\sigma_{sl}$, decreases and consequently it reduces the contact area (between liquid and solid surface) and therefore increases the height buildup of the nanoparticle ink line thus increasing the cross sectional area and the volume of deposited nanoparticles, this can consequently decreases the resistance of the printed line. It is therefore, essential to understand how concentration and characteristics of nanoparticles, base liquid, feasible nanoparticle coating, possible surfactant and the physical properties of the nanofluid affect the behavior of the triple line and hence the printing characteristics of a nanofluid ink on a particular substrate. The waviness or quality of the triple line [2,3] will be affected by characteristics of the solid substrate [4], distribution of nanoparticles in the triple region [5–7], force balance between liquid-gas [8–10] and solid surface tensions [11,12]. The liquid-gas and solid surface tensions play a significant role in the behavior of the triple line. Normally, the liquid-gas surface tension needs to remain within a certain range (0.028–0.033 N/m at operating temperature) to be printable using conventional inkjet printers. As a result, the force balance and quality of the triple line mainly depends on the solid surface tensions. The quality of the triple line has a significant influence on the resolution and resistance of printed lines and hence accurate characterization of the quality of the triple line is an important step in the development of a predictive capability for (3D) printing conductive lines.

In this study, the solid surface tensions are predicted, knowing the asymptotic contact angle for a solid-fluid pair, and the relations between solid surface tensions, printability of conductive nanoparticles and distribution of nanoparticles in the triple region are discussed. In addition, the distribution of nanoparticles and the layering phenomenon are examined for nanofluid drops on glass, polytetrofluoroethylene (PTFE) and stainless steel substrates using the environmental scanning electron microscopy (ESEM) technique for the first time.

2. The behavior of nanofluid triple lines

2.1. General behavior of triple lines

The liquid-gas, σ_{lg}, solid-liquid, σ_{sl}, and solid-gas, σ_{sg} surface tensions are major effective forces on the triple line. The schematic of liquid-gas and solid surface tensions, $\sigma_{sg}-\sigma_{sl}$, for droplets is given in Fig. 1. The liquid-gas surface tension is available for most chemicals however the solid-liquid and solid-gas surface tensions cannot be found easily. A couple correlations have been used to obtain the solid surface tensions [13,14], such as Berthelot's combining rule [15], the modified Berthelot's rule [16], the alternative formulation [17,18], and the equation of state formulation [19,20]. The correlations have been compared with each other for some materials [14]. For a given liquid-gas surface tension, the solid surface tensions can play a key role in the behavior of the triple line. It was observed that the radius of the triple line expands towards the gas phase as the solid surface tension increases [3].

Young equation, $\sigma_{lg}\cos\theta_e=\sigma_{sg}-\sigma_{sl}$, demonstrates the force balance between liquid-gas, σ_{lg}, and solid surface tensions, $\sigma_{sg}-\sigma_{sl}$, at the triple line, where the equilibrium contact angle, θ_e, is size independent (see Fig. 1). The Young equation has several limitations and has never been verified experimentally for axisymmetric droplets. The application of the Young equation is limited to ideal substrates [13,21] and contact angle is size independent [12,22] such as long droplets [12]. In the case of an axisymmetric droplet, one side of the Young equation, $\sigma_{lg}\cos\theta_e$, is size dependent while the other side of the equation, $\sigma_{sg}-\sigma_{sl}$, contains physical properties which makes the equation inconsistent.

It has been observed that the droplet contact angle varies under different gravitational accelerations based on the parabolic flight campaign [23] and drop tower methods [24]. It has been observed that droplet contact angle increases as the effect of gravity decreases. As the gravitational acceleration decreases to zero, the droplet shape gradually changes to a spherical cap. The droplet contact angle under zero gravity has been defined as the asymptotic contact angle, θ_s [11,12]. The asymptotic contact angle is only dependent on the physical properties and interactions between gas, liquid and solid at the triple line, and is a unique criterion to measure surface wettability or the effects of nanoparticles on surface wettability.

The contact angle has been observed to change with droplet volume [12,13,22], so the concept of line tension has been employed to explain the variation of droplet contact angle with volume. The line tension has a significant role in the effect of droplet size on contact angle, leading to a modified Young equation, $\frac{\sigma}{r_d}+\sigma_{lg}\cos\theta_e=\sigma_{sg}-\sigma_{sl}$ß, that considers the effect of the line tension, σ. The value of line tension has been obtained experimentally [13,25] and theoretically [26,27]. The line tension operates to expand the length of the triple line when it is negative and vice versa [25]. Most probably, the line tension would be zero under zero gravity conditions, since droplet contact angle, liquid-gas and solid surface tensions are constant while the radius of triple line would change by volume. It has been also reported that (a) the line tension decreases as wettability increases and likely vanishes at super-wetting [28], (b) the line tension is a function of the liquid material [28–31], (c) there are large uncertainties, associated with determining both magnitude and sign of the line tension [13,32]. The accurate measurement of line tension is difficult, because (I) its value is small, (II) lack of accurate measurement techniques, (III) possible contamination in triple line, (IV) lack of accurate modeling techniques and (V) the effect of various parameters on line tension is not well recognized

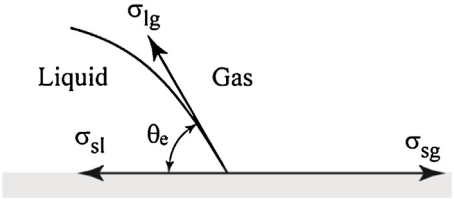

Fig. 1. Schematic of forces between liquid-gas and solid surface tensions at the droplet triple line.

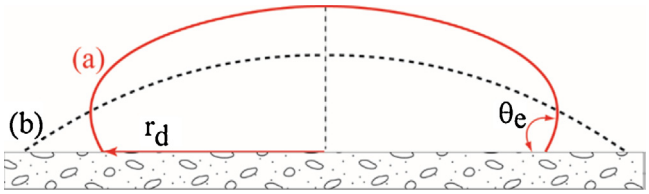

Fig. 2. Schematic of (a) wet (dash line) and (b) non-wet (solid line) droplets on substrate.

yet. Therefore, further studies are essential to better understand the line tension and the parameters that affect its magnitude and sign.

The characteristics of a solid surface [33] such as the homogeneity, roughness and material [34] have a significant effect on the behavior of the triple line [35–38] and contact angle hysteresis. The effect of surface roughness on contact angle have been considered in the Wenzel and Cassie-Baxter equations [35–38]. The uncertainties of the estimation [40,41] and the use of the correct form of these equations have been discussed in detail in reference [4].

For printable nanofluids, the presence of nanoparticles in the base liquid will potentially affect the roughness and homogeneity of solid substrates [39], the liquid-gas [8–10] and solid surface tensions [11], the disjoining pressure [5] and consequently the quality of the triple line. This will be discussed in the next section.

2.2. The effects of nanoparticles on the behavior of the triple line

The affinity of liquids for solid substrates is referred to as the wettability of the liquid [21]. Liquids with weak affinities for a solid substrate will minimize the radius of the triple line (see Fig. 2a) while those with high affinities for the solid surface will form films to maximize the radius of the triple line (see Fig. 2b) and consequently the liquid-solid contact area. For a given droplet volume, the droplet contact angle decreases with expansion of the radius of the triple line. The force balance between liquid-gas and solid surface tensions at the triple line (see Fig. 1) plays a key role in the behavior of the triple line. Practically, the characteristics of the nanoparticles have significant effects on the liquid-gas [8–10] and solid surface tensions [11] and the force balance at the triple line, which could consequently influence the radius of the triple line [2] and contact angle [42].

The effects of substrate, concentration and size of bismuth telluride nanoparticles (2.5 nm, 10.4 nm) on the behavior of the triple line have been discussed previously [8]. It was seen that the droplet contact angle increased with concentration of the nanoparticle for a given droplet volume, however, as the nanofluid concentration increased further ($\geq$0.02 w% for 2.5 nm nanoparticle size and $\geq$0.005 w% for 10.4 nm nanoparticle size), the droplet contact angle began to decrease. The liquid-gas surface tension was seen to reduce by more than 50% for a 2.5 nm bismuth telluride suspension. The accumulation and assembly of nanoparticles at the liquid-gas interface was assumed to be responsible for the dependence

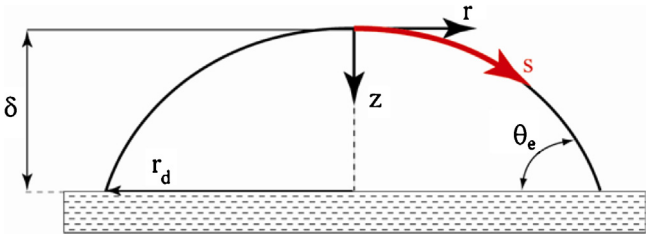

Fig. 3. Schematic of a droplet shape on solid substrate.

of the liquid-gas surface tension on nanoparticle concentration. More nanoparticles were driven to the liquid-gas interface region as the concentration of bismuth telluride in the nanofluid increased. The nanoparticles are bounded at the interface [43]. The liquid-gas surface tension decreased as results of electrostatic repulsion and the lower surface energy of the effective interface containing nanoparticle-water, nanoparticle-air and air-water surfaces compare with the original air-water interface. Variation of triple line has been observed to be greater with smaller nanoparticles [8]. In contrast, the effect of nanoparticles on the liquid-gas surface tension for aluminum-ethanol [9] and alumina-water [10] nanofluids has been reported to be negligible or weak. It has also been noted that nanoparticles in the vicinity of the triple line could enhance the wetting speed at low particle concentrations (smaller than 1 w%) in an investigation of the evaporation and spreading of aluminum-ethanol nanofluid on a hydrophobic Teflon-AF coated substrate [9]. The observed results were explained by the effects of nanoparticles on viscosity and disjoining pressure. It was proposed that the disjoining pressure would drive the spreading of the nanofluid however, at concentrations higher than 1 w%, the viscous forces dominate the disjoining pressure [9]. The triple line was shown to display a stick-slip behavior in a study of the evaporation and de-wetting behavior of an ethanol-titanium oxide nanofluid droplet on PTFE (1 μm thick PTFE layer on silicon wafer substrate) [44]. This behavior was attributed to deposited nanoparticles and/or an increase in viscosity in the triple region due to high local nanoparticle concentrations. In contrast, a continuous movement of the triple line was observed during the evaporation of a pure ethanol droplet. The effect of particle size on the pinning behavior of the evaporating droplets (5 μl droplet volume and 0.5 v% concentration nanofluid) has also been investigated [45], employing 2 nm gold, 30 nm copper oxide (CuO) and 11 and 47 nm alumina nanoparticles. It was reported that the particle size had a more significant effect on the dried stain pattern than the temperature of the substrate. Smaller particles resulted in a more uniform central deposition, whereas larger nanoparticles produced more deposited particles at the edge. It has also been observed that the shape and thickness of the deposited nanoparticles could be controlled by the speed of the evaporation [46,47]. In summary, it has been demonstrated in the literature that nanofluid characteristics, such as concentration, nanoparticle size and the base liquid have a significant impact on nanoparticle deposition and the quality of printed lines. The constituent parts of nanofluid inks for jet printing will be discussed in more detail in the next section.

2.3. Nanofluid inks

Conductive nanoparticles are mixed with base liquids to create inks for printing conductive lines. Sometimes the nanoparticles are coated to prevent agglomeration and the base liquids are mixed with surfactant to modify the viscosity and liquid-gas surface tension. Many nanofluid inks have been developed on this basis, such as 45 w%, 10 nm silver nanoparticle aqueous ink with the addition of the co-polymer, Pluronic F127 [48]. It was found in this case that the Pluronic F127 was effective not only as a stabilizer but also as a segregator aid, which stimulated the breakage of the agglomerated nanoparticles.

The strong tendency of nanoparticles to agglomerate is one of the most important issues in the formulation of stable and printable inks [49]. To this end an anionic polyelectrolyte has been employed as both capping agent and dispersant to produce a 25 w% aqueous silver nanofluid ink (10 nm–30 nm) [50]. The resultant nanofluid exhibited good long-term stability which was attributed to the electrosteric repulsion characteristic of the anionic polyelectrolyte [50]. Similarly, a poly (acrylic acid) sodium salt (PAA) was used to raise the stability of a 25 w% aqueous silver nanofluid inks (20 nm) [51].

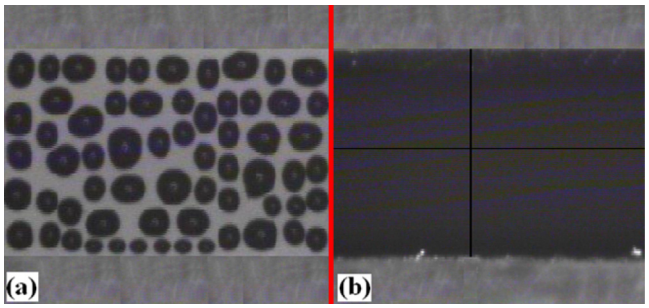

Fig. 4. Silver ink printed line on smooth (a) PTFE and (b) glass substrates.

20 nm silver nanoparticles have been mixed with two different base liquids (32 w%), triethylene glycol monomethyl ether (TGME) and ethanol to examine the effects of evaporation rate. The boiling temperature of TGME and ethanol respectively are 255 and 78.4 °C [52]. The surface wettability of the Si wafer substrate was controlled by a hydrophobic fluorocarbon (FC) film coating followed by UV/O_3 treatment. The results showed that droplet spreading was mainly dependent on wettability, evaporation rate and substrate temperature. For both inks, continuous lines were not produced on hydrophobic substrates at room temperature, however the continuity of injected lines improved with surface temperature. The continuity of injected lines with ethanol-based inks was much better than that of TGME-based inks.

Mixtures of carboxylate-modified polystyrene fluorescent beads of 100 nm and 1.1 μm in DI-water (0.5 v%) have been used to study the effects of particle size during the drying process [53,54]. For a given volume fraction, the total number of nanoparticles is much larger than that of microparticles and the nanoparticles can become closer to the triple line, which facilitates pinning of the triple line. In another study, a copper hexanoate in chloroform nanofluid was used to investigate copper lines deposited on glass. It was observed that the height, width and profile of the dried copper hexanoate lines changed with concentration and that as concentration decreases, less solute deposits at the triple line increasing the de-pinning effects.

In general, it can be seen that the characteristics and concentration of nanoparticles and the physical properties of the base liquid and any surfactant have an important influence on the physical properties of a nanofluid. Furthermore, the physical properties of the nanofluid, solid substrate and surrounding gas have a significant effect on the formation of injected droplets, the behavior of the triple line and consequently the quality of printed lines. The quality of triple line also depends on the distribution of nanoparticles on triple region, which is discussed in the next section.

2.4. Layering phenomenon in triple region

The distribution of particles in the triple region has potential impact on the spreading and quality of the triple line, hence, there have been several attempts to observe the distribution of particles using optical methods. Experimental evidence has revealed that nanoparticles might form an ordered structure in the triple region of a droplet on a solid substrate [5,6]. It has been observed that the number of layers of nanoparticles decreases in a stepwise pattern towards the triple line edge. This layering phenomenon has been demonstrated for a 19 nm silica nanofluid (10 v%) film formed between an oil drop and a solid surface, using reflected light interferometry.

A microscopy technique has been developed utilizing an objective with a high magnification (90×) to observe the spontaneous spreading of nanofluids on a glass substrate from the top view with another lens used to see the profile of droplet from the side view simultaneously [55]. The rate of spreading of a nanofluidic film was observed as a function of concentration (5, 10 and 20 v%) with 19 nm silica nanoparticles in an oil drop. Employing this optical technique, two distinct lines were observed in the triple region. The first one was the outer conventional contact line and the second one was an inner contact line formed by the nanofluid film between the oil drop and the solid surface. It was seen that the structural disjoining pressure, and hence rate of spreading, increased with concentration whilst the rate of spreading decreased with decreasing drop volume. This is because as drop volume decreases the capillary pressure increases whilst the structural disjoining pressure is constant.

The 1D Young–Laplace equation has been modified by introducing the disjoining pressure [7]. The modified equation predicted that the displacement of the contact line increases with: increased nanoparticle concentration, decreased particle size, mono rather than poly-dispersion, decreased resisting capillary pressure, decreased interfacial tension and increased radius of dispersed drop/bubble. Similar results have been obtained when modifying the 2D Young–Laplace equation by adding the effect of disjoining pressure [56].

The existing evidence indicates that the force balance between interfacial surface tension and solid surface tensions has a significant role in the spreading of a nanofluid on a solid substrate. In addition, it has been shown that particles can displace the triple line to a distance of 20–50 times of particle diameter as results of structural disjoining pressure and self-ordering of particles in a triple region. The disjoining pressure becomes effective at relatively high particle concentrations, i.e. over 20 v% [7].

3. Experimental setup

In order to create a nanofluid ink (Silverjet DGP-40LT-15C) with 38.853 w% 30–40 nm silver nanoparticles were mixed with Triethylene Glycol Monoethyl Ether (TGME). A Dimatix printer with nozzle size 21.5 μm was used to print conductive lines on glass and PTFE substrates. The roughness of the substrates was measured using an interferometry method. The roughness of glass and PTFE substrates were respectively 55.3 nm and 100 nm.

A Kruss contact angle meter (Drop Shape Analysis System DSA100) was employed to measure the liquid-gas surface tension of the silver nanofluid and characterize the shape of nanofluid droplets in and equilibrium condition. The liquid-gas surface tension of the silver ink was found to be 0.0235 ± 0.0005 N/m. Knowing the liquid-gas surface tension and the droplet dimensions in equilibrium condition, the solid surface tensions could be determined. The method used to calculate the solid surface tensions is described in Section 4.2.

An environmental scanning electron microscope (ESEM) was employed to investigate the effects of solid substrate and droplet size on the distribution of silver nanoparticles in the nanofluid and observe the layering phenomenon. These experiments are discussed in Section 5.

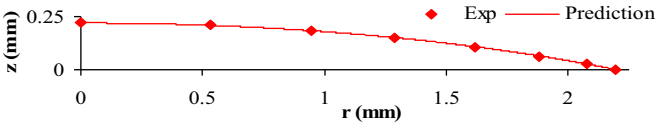

Fig. 5. Comparison between experimental and predicted droplet shape.

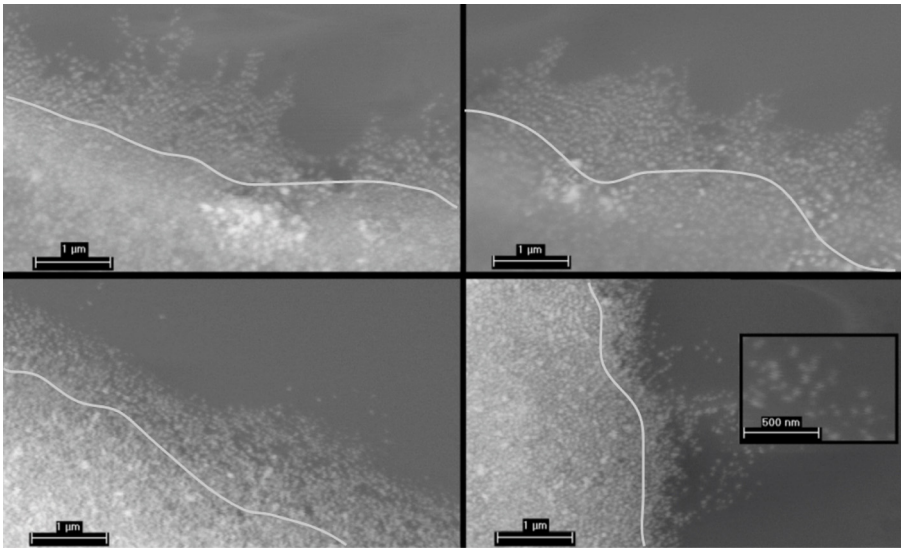

Fig. 6. Distribution of 30–40 nm silver nanoparticles in triple region on glass substrate.

4. Theoretical analysis

4.1. Prediction of droplet shape

The Young–Laplace equation has been solved to predict bubble [58–61] and droplet [11,12,42] shapes. The Young–Laplace equation represents the equilibrium between two fluids, separated by an interface, and gives the pressure difference across the liquid-gas interface as a function of the product of the curvature multiplied by the liquid-gas surface tension. R_1 and R_2 are the radii of the curvature at the liquid-gas interface, where R_1 is the radius of curvature describing the latitude as it rotates and R_2 is the radius of curvature in a vertical section, describing the longitude as it rotates. The centres of R_1 and R_2 are on the same line, vertical to the liquid-gas interface. The Young–Laplace equation can be applied under a quasi-steady state condition, where the static pressure and surface tension forces are the only effective elements and there is equilibrium between gas and liquid at the interface. In general, the Young–Laplace can be used to predict a droplet shape while the effects of inertia and viscosity are negligible with respect to the liquid-gas surface tension force. The Young–Laplace equation can be written as

$$\Delta p = \left(\frac{1}{R_1} + \frac{1}{R_2}\right)\sigma_{lg} \tag{1}$$

where Δp is the pressure difference between the gas, $p_g(z)$, and liquid, $p_l(z)$, which can be defined as, $p_g(z) = \rho_g g z$, and $p_l(z) = \frac{2\sigma_{lg}}{R_o} + \rho_l g z$, where g and R_o are respectively are gravitational acceleration and radius of curvature at the apex respectively.

Knowing the pressure difference between the gas and liquid phases, the Young–Laplace equation can be written as

$$\frac{d\theta}{ds} = \frac{2}{R_o} + \frac{gz}{\sigma_{lg}}(\rho_l - \rho_g) - \frac{\sin\theta}{r} \tag{2}$$

In the case of nanofluids, the liquid-gas surface tension, σ_{lg}, should be substituted by the liquid-gas surface tension of the nanofluid, σ_{lgn}. The Young–Laplace equation can be solved, with the following system of ordinary differential equations for axisymmetric interfaces, to obtain the droplet shape (see Fig. 3)

$$\frac{dr}{ds} = \cos\theta \tag{3}$$

$$\frac{dz}{ds} = \sin\theta \tag{4}$$

$$\frac{dV}{ds} = \pi r^2 \sin\theta \tag{5}$$

This system of ordinary differential equations avoids the singularity problem at the droplet apex, since

$$\left.\frac{\sin\theta}{r}\right|_{s=0} = \frac{1}{R_o} \tag{6}$$

Using the Runge–Kutta method, the system of ordinary differential Eqs. (2)–(5) can be solved [7,8,31] to predict the shape and characteristics of the droplet (radius of curvature at apex, R_o, equilibrium contact angle, θ_e, and volume), knowing the radius of the triple line, r_d, droplet height, δ, (see Fig. 3) and applying the following boundary conditions

$$r(0) = z(0) = \theta(0) = V(0) = 0. \tag{7}$$

4.2. Determination of solid surface tensions

The droplet shape depends on the liquid-gas-solid materials and gravity. The droplet contact angle has been observed to increase as gravity decreases [23,24]. Eventually, the droplet profile attains the shape of a spherical cap under conditions of zero gravity. The contact angle under these conditions is called the asymptotic contact angle, θ_s. Under zero gravity, assuming the substrate is smooth and homogenous, the force balance at the triple line can be expressed precisely by the following modified form of the Young equation

$$\sigma_{lg}\cos\theta_s = \sigma_{sg} - \sigma_{sl}. \tag{8}$$

The asymptotic contact angle can be determined from experiments in which droplet volume is gradually reduced [12]. The effect of gravity decreases with reduction of droplet volume and consequently the contact angle increases [13,22]. The asymptotic contact angle can be obtained theoretically [11,12], using the characteristics of droplets under normal gravitational conditions.

As indicated by the following hypothesis from reference [12], '*For given liquid, gas and solid materials, the interfacial force on a droplet, normal to the solid surface, is uniquely defined; in particular, this force is independent of the acceleration of gravity*'. This means the

normal component of the droplet interfacial force is independent of gravity and the following equation can be derived

$$r_d \sin\theta_e = \left[\frac{3V}{\pi(2+\cos\theta_s)(1-\cos\theta_s)^2}\right]^{1/3} \sin^2\theta_s \quad (9)$$

The asymptotic contact angle, θ_s, can then be calculated from Eq. (9), knowing the characteristics of a droplet, such as radius of triple line, r_d, equilibrium contact angle in normal gravity, θ_e, and droplet volume, V. The solid surface tensions can then be calculated from Eq. (8), knowing the asymptotic contact angle, θ_s. The system of ordinary differential Eqs. (2)–(5) along with Eq. (9) can, hence, be solved to predict the droplet shape, knowing only one droplet characteristic such as the radius of the triple line, contact angle, droplet height or droplet volume [11,12].

5. Results and discussion

5.1. Calculation of solid surface tension and prediction of droplet shape

The silver ink droplet shape on a smooth substrate was captured using the Drop Shape Analysis System DSA100. Knowing the characteristics of a droplet, Eq. (9) was solved to predict the asymptotic contact angle, θ_s. Having the asymptotic contact angle and liquid-gas surface tension, the solid surface tensions could be calculated from Eq. (8). The solid surface tensions for glass and PTFE substrates were hence determined to be 0.0228 N/m and 0.0043 N/m respectively for the silver ink used. The experimental uncertainty for the measurement of solid surface tensions was estimated to be less than 6%. The solid surface tensions value for the PTFE substrate is relatively low and consequently the silver ink demonstrated poor wettability of the PTFE, resulting in a series of disconnected droplets, as shown in Fig. 4(a). In contrast the relatively high solid surface tensions value with the glass substrate resulted in high wettability of the silver ink, as shown in Fig. 4(b).

Fig. 5 compares the experimental data with predicted droplet shape. The latter obtained from solving the system of ordinary differential Eqs. (2)–(5) along with Eq. (9) and the boundary conditions given by Eq. (7), knowing only the droplet volume and physical properties. The percentage of absolute errors between theoretical prediction and experimental data for points 1–8 respectively were 0.79, 0.01, 0.67, 0.49, 0.38, 0.67, 0.61 and 0.4. Point 8 has maximum radius of triple line. The good agreement between experimental data and theoretical prediction indicates the accuracy of Eq. (9).

5.2. Printability of the silver ink

The quality of the printed lines on smooth glass was observed to be reasonable. The good quality of the printed line is attributed to the relatively high value of the solid surface tensions, since the liquid-gas surface tension of the nanofluid remained in the range 0.028–0.033 N/m. Therefore, the affinity of a nanofluid ink for a solid substrate depends principally on the solid surface tensions. As the solid surface tension value increases, injected nanofluid drops have an increasing tendency to spread over the substrate and create continuous lines, as long as the substrate is sufficiently smooth. However, in the case of a rough substrate, the injected nanofluid drops tend to spread along scratches, thus reducing the quality of the triple line and the resolution of the printed line. As the solid surface tensions value decreases, the injected nanofluid drops tend to create discrete drops rather than the desired continuous line. The solid surface tensions value can, therefore, be seen as a reliable criterion to measure the printability of conductive nanofluids on substrates, since the effects of gas, liquid and solid need to be considered all together.

5.3. Nanoparticle distribution at the triple line

The distribution of nanoparticles in the triple region is an important factor in the resolution and resistivity of printed line when using nanofluids with conductive nanoparticles. The optical evidence has indicated a layering phenomenon for the nanoparticles in the triple region [5,6,55–57]. In this research, ESEM was used to observe the distribution of silver nanoparticles in the triple region for silver ink droplets on a glass substrate. Fig. 6 shows four images of the distribution of 30–40 nm silver nanoparticles in the triple region in the liquid phase. It can be seen that beyond the dotted line the nanoparticles are layered and the nanoparticles appeared to have extended the triple line in a non-uniform fashion with the formation of 'fingers'. This can be attributed to the structural disjoining pressure and nanoparticle self-assembly discussed previously. This irregular triple line and associated irregular nanoparticle distribution is potentially detrimental to the edge definition of printed lines. To investigate this further, Fig. 7 shows the distribution of the silver nanoparticles on a glass substrate after the silver nanofluid has dried. It can be seen that the distribution of nanoparticles after drying is consistent with the distribution of the nanoparticles in the triple region in the liquid phase. This indicates the importance of the distribution of nanoparticles at the triple line in the liquid phase on the final distribution of nanoparticles and, hence, quality and resolution of printed lines.

It was observed that the surfactant inside the silver nanofluid spread beyond the triple line on the substrate when silver nanofluid droplets were left on the glass substrate for a long time (more than 6 h). This is because the liquid with the greater affinity with the substrate tends to separate from the base liquid and spread out on the substrate. The segregated liquid can carry the smaller nanoparticles and the presence of small nanoparticles in the segregated liquid on the substrate was observed. However, the segregation of surfactant and base liquid was seen to be negligible in small droplets ($r_d \leq 0.5$ mm) as the outward solid surface tensions force depends on the length of the triple line and as a result, more segregation occurs in bigger droplets ($r_d > 2.5$ mm). The segregation of surfactant from the base liquid has a positive impact on the spreading of nanoparticles in the triple region. Similarly, for a given silver nanofluid, the spreading of nanoparticles and layering phenomena for bigger droplets were more obvious. Even though the hydrostatic pressure is higher for smaller droplets (see Eq. (2)), since the radius of curvature at apex is lower, the effect of solid surface tensions force is more dominant for bigger droplets and as results, the spreading of nanoparticles is more obvious for big droplets.

Fig. 8 shows the distribution and spreading of silver nanoparticles in the triple region for the same silver ink on a stainless steel substrate. Layering of nanoparticles near the triple region and non-uniform spreading on the substrate were again observed, however, the nanoparticles spread less on stainless steel surface. This can be attributed to the lower affinity of the sliver nanofluid for the steel substrate. As indicated by the lower solid surface tensions value for the stainless steel, which was slightly less than that of glass but bigger than PTFE. Regions I and III in Fig. 8 were observed frequently, however, the 'finger' in Region II was only rarely observed. It can be seen that the nanoparticle density appears to be lower in Region II and would not form a continuous solid on sintering.

A similar experiment was also conducted with a PTFE substrate. In this case the layering of nanoparticles in the triple region was not seen, since the affinity of the silver nanofluid for PTFE was weak. In addition to disjoining pressure, the affinity of the nanofluid for the substrate has a significant role in spreading and distribution of nanoparticles in the triple region, since the nanoparticles are bound in the base liquid. As affinity of a nanofluid for the substrate increases, the nanoparticles have a greater tendency to spread over the substrate. In summary, it appears that the nanoparticles have

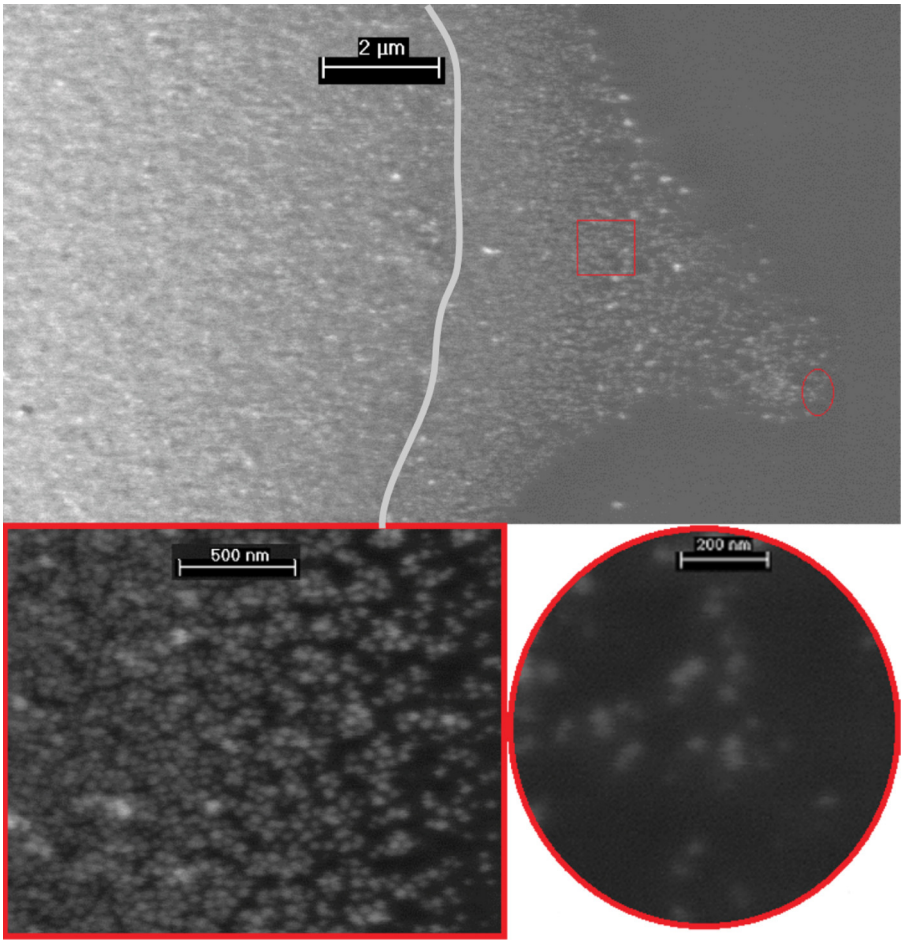

Fig. 7. Distribution of 30–40 nm silver nanoparticles on glass substrate after drying.

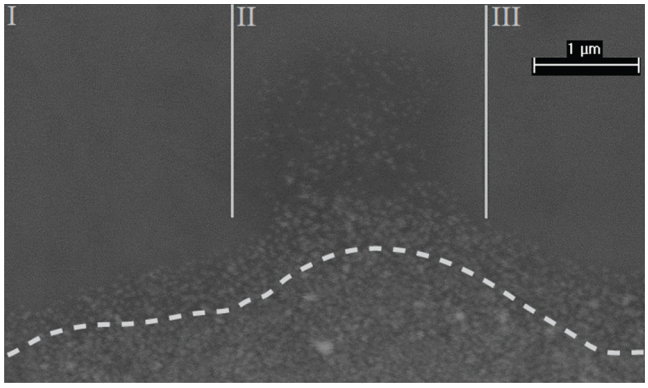

Fig. 8. Distribution of 30–40 nm silver nanoparticles in triple region on stainless steel substrate in the liquid phase.

two major roles on the spreading of a nanofluid; (a) in modifying the physical properties of the nanofluid, such as the liquid-gas and solid surface tensions and (b) changing the disjoining pressure. Both effects will impact the distribution and spreading of nanoparticles on a substrate.

6. Conclusions

The solid surface tensions for a silver nanofluid ink on glass and PTFE substrates were determined, after calculating the asymptotic contact angle. The solid surface tensions on glass and PTFE were respectively 0.0228 N/m and 0.00433 N/m. For a given ink, it was observed that the affinity of a liquid for a substrate increased with the value for the solid surface tensions. In fact, nanofluids with weak affinities for a solid substrate collect themselves into discrete droplets, while those with high affinities for the solid surface maximize the radius of triple line and make a continuous line. Hence, the value of the solid surface tensions can be used as a reliable criterion to measure the printability of a nanofluid on a solid surface. For a given nanofluid, as solid surface tensions increases, the quality of the printed lines on the substrate increases.

The silver nanofluid ink and glass substrate were found to be a suitable combination to study the distribution of nanoparticles in the triple region, using ESEM. ESEM was employed to study the distribution of silver nanoparticles in the triple region on glass, stainless steel and PTFE substrates. The distribution of nanoparticles and layering phenomenon were clearly observed on the glass substrate, since the silver nanofluid ink has a high affinity for the glass substrate. The distribution of nanoparticles observed after the nanofluid was dried on the glass substrate was seen to be consistent with that observed in the liquid phase. The effect of size of droplet on spreading of nanoparticles was examined and it was seen that the spreading of nanoparticles on the substrate increased with droplet size, which can be attributed to expansion of the length of the triple line and consequent enhancement of the solid surface tensions force. Similarly, the effect of substrate was investigated on the spreading of nanoparticles. In addition to disjoining pressure, the affinity of a nanofluid for a substrate was observed to have an impact on the spreading of nanoparticles. Unlike with glass and metal substrates, the layering phenomenon was negligible with

the PTFE substrate, since the affinity of the silver nanofluid ink was weak in this case.

Acknowledgments

The authors would like to extend thanks to EPSRC for financial support, members and the director of the EPSRC Centre for Innovative Manufacturing in Additive Manufacturing.

References

[1] S. Vafaei, C. Tuck, I. Ashcroft, R. Wildman, Surface microstructuring to modify wettability for 3D printing of nano-filled inks, Chem. Eng. Res. Des. (2016) (in press).
[2] S. Vafaei, D. Wen, The effect of gold nanoparticles on the spreading of triple line, Microfluid. Nanofluid. 8 (2010) 843–848.
[3] S. Vafaei, D. Wen, Spreading of triple line and dynamics of bubble growth inside nanoparticle dispersions on top of a substrate plate, J. Colloid Interface Sci. 362 (2011) 285–291.
[4] A.J.B. Milne, A. Amirfazli, The Cassie equation: how it is meant to be used, Adv. Colloid Interface Sci. 170 (2012) 48–55.
[5] D.T. Wasan, A.D. Nikolov, Spreading of nanofluids on solids, Nature 423 (2003) 156–159.
[6] A. Nikolov, K. Kondiparty, D. Wasan, Nanoparticle self-structuring in a nanofluid film spreading on a solid surface, Langmuir 26 (2010) 7665–7670.
[7] A. Chengara, D. Nikolov, D. Wasan, A. Trokhymchuk, D. Henderson, Spreading of nanofluids driven by the structural disjoining pressure gradient, J. Colloid Interface Sci. 280 (2004) 192–201.
[8] S. Vafaei, A. Purkayastha, A. Jain, G. Ramanath, T. Borca-Tasciuc, The effect of nanoparticles on the liquid-gas surface tension of Bi_2Te_3 nanofluids, Nanotechnology 20 (2009) 185702–185708.
[9] K. Sefiane, J. Skilling, J. MacGillivray, Contact line motion and dynamic wetting of nanofluid solutions, Adv. Colloid Interface Sci. 138 (2008) 101–120.
[10] S.J. Kim, I.C. Bang, J. Buongiorno, L.W. Hu, Surface wettability change during pool boiling of nanofluids and its effect on critical heat flux, Int. J. Heat Mass Transfer. 50 (2007) 4105–4116.
[11] S. Vafaei, D. Wen, T. Borca-Tasciuc, Nanofluids surface wettability through asymptotic contact angle, Langmuir 27 (2011) 2211–2218.
[12] S. Vafaei, M.Z. Podowski, Analysis of the relationship between liquid droplet size and contact angle, Adv. Colloid Interface Sci. 113 (2005) 133–146.
[13] A.W. Neumann, J.K. Spelt, Applied Surface Thermodynamics, M. Dekker, 1996.
[14] D.Y. Kwok, A.W. Neumann, Contact angle measurement and contact angle interpretation, Adv. Colloid Interface Sci. 81 (1999) 167–249.
[15] D. Berthelot, Sur le mélange des gaz, Comptes rendus hebdomadaires des séances de l'Académie des Sciences 126 (1898) 1703–1855.
[16] D. Li, A.W. Neumann, Reformulation of the equation of state for interfacial tensions, J. Colloid Interface Sci. 137 (1990) 304–307.
[17] D.Y. Kwok, A.W. Neumann, Contact angle interpretation in terms of solid surface tension, Colloid Surf. A Physicochem. Eng. Asp. 161 (2000) 31–48.
[18] D.Y. Kwok, Contact Angles and Surface Energetics, Ph.D Thesis, University of Toronto, 1998.
[19] O. Driedger, A.W. Neumann, P.J. Sell, An equation of state approach for surface free energies, Kolloid-Z. Z. Polym. 201 (1965) 52–57.
[20] A.W. Neumann, R.J. Good, C.J. Hope, M. Sejpal, An equation-of-state approach to determine surface tensions of low-energy solids from contact angles, J. Colloid Interface Sci. 49 (1974) 291–304.
[21] V.P. Carey, Liquid-vapor Phase-change Phenomena, second ed., Hemisphere Publishing Corporation, 2008.
[22] J. Gaydos, A.W. Neumann, The dependence of contact angles on drop size and line tension, J. Colloid Interface Sci. 120 (1987) 76–86.
[23] D. Brutin, Z.Q. Zhu, O. Rahli, J.C. Xie, Q. Liu, L. Tadrist, Sessile drop in microgravity: creation, contact angle and interface, Microgravity Sci. Technol. 21 (2009) 67–76.
[24] A. Diana, M. Castillo, D. Brutin, T. Steinberg, Sessile drop wettability in normal and reduced gravity, Microgravity Sci. Technol. 24 (2012) 195–202.
[25] P. Chen, S.S. Susnar, C. Mak, A. Amirfazli, A.W. Neumann, Lens size dependence of contact angle and the line tension of the dodecane-water-air system, Colloid Surf. A Physicochem. Eng. Asp. 129–130 (1997) 45–60.
[26] H. Hoorfar, A. Amirfazli, J.A. Gaydos, A.W. Neumann, The effect of line tension on the shape of liquid menisci near stripwise heterogeneous walls, Adv. Colloid Interface Sci. 114–115 (2005) 103–118.
[27] A. Marmur, Line tension and the intrinsic contact angle in solid-liquid-fluid systems, J. Colloid Interface Sci. 186 (1997) 462–466.
[28] A. Amirfazli, A. Keshavarz, L. Zhang, A.W. Neumann, Determination of line tension for systems near wetting, J. Colloid Interface Sci. 265 (2003) 152–160.
[29] A. Amirfazli, D. Chatain, A.W. Neumann, Drop size dependence of contact angles for liquid tin on silica surface: line tension and its correlation with solid-liquid interfacial tension, Colloid Surf. A Physicochem. Eng. Asp. 142 (1998) 183–188.
[30] D. Duncan, D. Li, J. Gaydos, A.W. Neumann, Correlation of line tension and solid-liquid interfacial tension from the measurement of drop size dependence of contact angles, J. Colloid Interface Sci. 169 (1995) 256–261.
[31] A. Amirfazli, D.Y. Kwok, J. Gaydos, A.W. Neumann, Line tension measurements through drop size dependence of contact angle, J. Colloid Interface Sci. 205 (1998) 1–11.
[32] A. Amirfazli, A.W. Neumann, Status of the three-phase line tension, Adv. Colloid Interface Sci. 110 (2004) 121–141.
[33] L. Gao, T.J. McCarthy, Wetting, Langmuir 24 (2009) 14105–14115.
[34] C. Antonini, A. Amirfazli, M. Marengo, Drop impact and wettability: from hydrophilic to superhydrophobic surfaces, Phys. Fluids 24 (2012) (1021041-13).
[35] A.B.D. Cassie, Disc Faraday Soc. 3 (1948) 11–16.
[36] S. Baxer, A.B.D. Cassie, J. Text. Inst. 36T (1945) 67–90.
[37] A.B.D. Cassie, S. Baxter, Trans. Faraday Soc. 40 (1944) 546–551.
[38] G. Wolansky, A. Marmur, Apparent contact angles on rough surfaces: the Wenzel equation revisited, Colloid Surf. A Physicochem. Eng. Asp. 156 (1999) 381–388.
[39] S. Vafaei, T. Borca-Tasciuc, Role of nanoparticles in nanofluid boiling: nanoparticle deposition, Chem. Eng. Res. Des. (2016) (in press).
[40] L. Gao, T.J. McCarthy, How Wenzel and Cassie were wrong, Langmuir 23 (2007) 3762–3765.
[41] L. Gao, T.J. McCarthy, An attempt to correct the faulty intuition perpetuated by the Wenzel and Cassie laws, Langmuir 25 (2009) 7249–7255.
[42] S. Vafaei, T. Borca-Tasciuc, M.Z. Podowski, A. Purkayastha, P.G. Ramanath, P.M. Ajayan, Effect of nanoparticles on sessile droplet contact angle, Nanotechnology 17 (2006) 2523–2527.
[43] J. Ally, M. Kappl, H.J. Butt, A. Amirfazli, Detachment force of particles from air-liquid interfaces of films and bubbles, Langmuir 26 (2010) 18135–18143.
[44] J.R. Moffat, K. Sefiane, M.E.R. Shanahan, Effect of TiO_2 nanoparticles on contact line stick-slip behavior of volatile drops, J. Phys. Chem. B 113 (2009) 8860–8866.
[45] C.H. Chon, S. Paik, J.B. Tipton, K.D. Kihm, Effect of nanoparticle sizes and number densities on the evaporation and dryout characteristics for strongly pinned nanofluid droplets, Langmuir 23 (2007) 2953–2960.
[46] R.D. Deegan, O. Bakajin, T.F. Dupont, G. Huber, S.R. Nagel, T.A. Witten, Capillary flow as the cause of ring stains from dried liquid drops, Nature 389 (1997) 827–829.
[47] R.D. Deegan, O. Bakajin, T.F. Dupont, G. Huber, S.R. Nagel, T.A. Witten, Contact line deposits in an evaporating drop, Phys. Rev. E 62 (1) (2000) 756–765.
[48] A. Kosmala, Q. Zhang, R. Wright, P. Kirby, Development of high concentrated aqueous silver nanofluid and inkjet printing on ceramic substrates, Mater. Chem. Phys. 132 (2012) 788–795.
[49] A. Kosmala, R. Wright, Q. Zhang, P. Kirby, Synthesis of silver nanoparticles and fabrication of aqueous Ag inks for inkjet printing, Mater. Chem. Phys. 129 (2011) 1075–1080.
[50] S. Jeong, H.C. Song, W.W. Lee, Y. Choi, S.S. Lee, B.H. Ryu, Combined role of well-dispersed aqueous Ag ink and the molecular adhesive layer in inkjet printing the narrow and highly conductive Ag features on a glass substrate, J. Phys. Chem. C 114 (2010) 22277–22283.
[51] S. Jeong, H.C. Song, W.W. Lee, Y. Choi, B.H. Ryu, Preparation of aqueous Ag Ink with long-term dispersion stability and its inkjet printing for fabricating conductive tracks on a polyimide film, J. Appl. Phys. 108 (2010) 1028051–1028055.
[52] K.Y. Shin, S.H. Lee, J.H. Oh, Solvent and substrate effects on inkjet-printed dots and lines of silver nanoparticle colloids, J. Micromech. Microeng. 21 (2011) (045012 1-11).
[53] V.H. Chhasatia, Y. Sun, Interaction of bi-dispersed particles with contact line in an evaporating colloidal drop, Soft Matter 7 (2011) 10135–10143.
[54] T. Cuk, S.M. Troian, C.M. Hong, S. Wagner, Using convective flow splitting for the direct printing of fine copper lines, Appl. Phys. Lett. 77 (2000) 2063–2065.
[55] K. Kondiparty, A.D. Nikolov, D. Wasan, K.L. Liu, Dynamic spreading of nanofluids on solids, part I: experimental, Langmuir 28 (2012) 14618–14623.
[56] K. Kondiparty, A.D. Nikolov, S. Wu, D. Wasan, Wetting and spreading of nanofluids on solid surfaces driven by the structural disjoining pressure: statics analysis and experiments, Langmuir 27 (2011) 3324–3335.
[57] D. Wasan, A. Nikolov, K. Kondiparty, The wetting and spreading of nanofluids on solids: role of the structural disjoining pressure, Curr. Opin. Colloid Interface Sci. 16 (2011) 344–349.
[58] S. Vafaei, D. Wen, Effect of gold nanoparticles on the dynamics of gas bubbles, Langmuir 26 (2010) 6902–6907.
[59] S. Vafaei, D. Wen, Bubble formation in a quiescent pool of gold nanoparticle suspension, Adv. Colloid Interface Sci. 159 (2010) 72–93.
[60] S. Vafaei, P. Angeli, D. Wen, Bubble growth rate from stainless steel substrate and needle nozzles, G, Colloid Surf. A Physicochem. Eng. Asp. 387 (2011) 240–247.
[61] S. Vafaei, T. Borca-Tasciuc, D. Wen, Theoretical and experimental investigation of quasi-steady-state bubble growth on top of submerged stainless steel nozzles, Colloid Surf. A Physicochem. Eng. Asp. 369 (2010) 11–19.